energies

MDPI

Article

Exergy Flows inside a One Phase Ejector for Refrigeration Systems

Mohammed Khennich, Mikhail Sorin * and Nicolas Galanis

Department of Mechanical Engineering, Université de Sherbrooke, Sherbrooke, QC J1K 2R1, Canada; Mohammed.Khennich@USherbrooke.ca (M.K.); Nicolas.Galanis@USherbrooke.ca (N.G.)
* Correspondence: Mikhail.V.Sorin@usherbrooke.ca; Tel.: +1-819-821-8000

Academic Editor: Jean-Pierre Bédécarrats
Received: 2 February 2016; Accepted: 14 March 2016; Published: 17 March 2016

Abstract: The evaluation of the thermodynamic performance of the mutual transformation of different kinds of exergy linked to the intensive thermodynamic parameters of the flow inside the ejector of a refrigeration system is undertaken. Two thermodynamic metrics, exergy produced and exergy consumed, are introduced to assess these transformations. Their calculation is based on the evaluation of the transiting exergy within different ejector sections taking into account the temperature, pressure and velocity variations. The analysis based on these metrics has allowed pinpointing the most important factors affecting the ejector's performance. A new result, namely the temperature rise in the sub-environmental region of the mixing section is detected as an important factor responsible for the ejector's thermodynamic irreversibility. The overall exergy efficiency of the ejector as well as the efficiencies of its sections are evaluated based on the proposed thermodynamic metrics.

Keywords: ejector; efficiency; exergy produced; exergy consumed; refrigeration

1. Introduction

Ejector-based refrigeration systems may be an attractive solution wherever low-grade thermal energy (industrial waste heat or solar energy) is available. Among their advantages are the simplicity in construction, installation and maintenance. However one of the most important shortcomings of these systems is their relatively low coefficient of performance (COP) [1]. To understand the main causes of this inefficiency some authors [2–4] have undertaken second law thermodynamic analysis of ejectors. Arbel *et al.* [2] performed an analysis of entropy generation within ejectors. Al-Najem *et al.* [3] presented one of the possible definitions of ejector exergy efficiency. McGovern *et al.* [4] showed that many performance measures of ejectors efficiency can be used, but they have not always been clearly defined and the rationale underlying and justifying these measures was often unclear. They also illustrated that the common ground for assessing ejectors performance was to define thermodynamically reversible reference processes against which real processes may be benchmarked. These reversible processes represent the thermodynamic limit of real ejector performance. However the authors proved that even for the relatively simple case of fixed conditions for two identical inlet fluids, 21 reversible reference processes were possible.

In the present paper, a new systematic methodology is proposed to define the efficiency of an ejector and its parts independently of a chosen reversible reference process. The methodology is based on the computation of the transiting exergy flow through a thermodynamic system, a concept first introduced by Brodyansky *et al.* [5]. Two important metrics arise from this analysis, the exergy production and exergy consumption in different parts of the ejector. In the case of identical inlet fluids, analysed in the present paper, each of these metrics is linked to three intensive parameters of the flow inside the ejector, namely pressure, temperature and velocity.

2. Transiting Exergy in a Process with Pressure, Temperature and Velocity Variations

The Grassmann diagram in Figure 1 illustrates a thermodynamic process where the intensive properties, such as temperature (T), pressure (P) and velocity (V) of a material stream change from their inlet (in) to outlet (out) values. The widths of the bands present the inlet and outlet exergies. The difference between these widths is the lost exergy (D). The specific exergy is defined as $e(P, T, V) = \left(\left[h + 0.5V^2\right] - h_0\right) - T_0.(s - s_0)$. The Grassmann exergy efficiency is defined in the Equation (1) as follows:

$$\eta_{ex,GR} = E_{out}/E_{in} = 1 - (D/E_{in}) \tag{1}$$

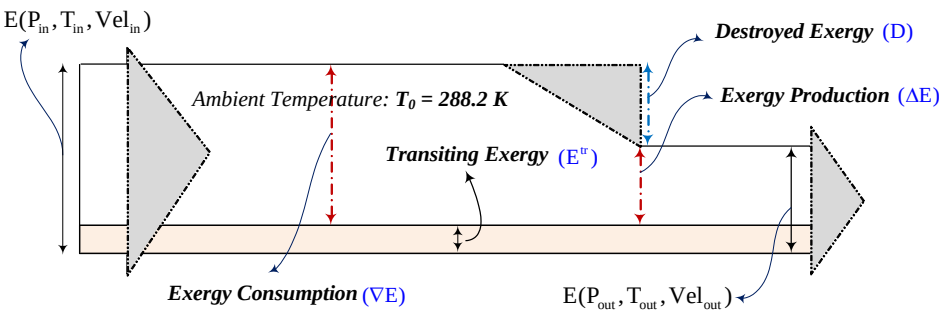

Figure 1. Grassmann diagram with transiting exergy.

According to Brodyansky *et al.* [5], the transiting exergy of material stream is the lowest exergy value defined by the intensive parameters at the inlet and the outlet of an analysed system or its parts. The following equations illustrate the computation of transiting exergy:

$$\text{If}\,(T_{in} > T_0 \text{ and } T_{out} > T_0) : E^{tr} = E(P_{min}, \mathbf{T}_{min}, V_{min}) \tag{1a}$$

$$\text{If}\,(T_{in} < T_0 \text{ and } T_{out} < T_0) : E^{tr} = E(P_{min}, \mathbf{T}_{max}, V_{min}) \tag{1b}$$

$$\text{If}\,(T_{in} > T_0 \text{ and } T_{out} < T_0)\,\text{OR}\,(T_{in} < T_0 \text{ and } T_{out} > T_0) : E^{tr} = E(P_{min}, \mathbf{T}_0, V_{min}) \tag{1c}$$

These equations illustrate the fact that this lowest value of exergy is defined by the minimum values of pressure and velocity chosen among their inlet and outlet values. The situation is quite different for temperature since the transiting exergy is defined by its minimum value if the inlet and outlet conditions are higher than the environmental temperature T_0, Equation (1a), by its maximum value for sub-environmental conditions, Equation (1b) and by the value T_0 if the environmental temperature has an intermediate value, Equation (1c). Figure 1 visualises the fact that the introduction of the transiting exergy results in a shift of the reference state for exergy calculations. As a result the exergy consumed and produced in a system or its parts are represented by smaller band widths.

The "transiting exergy approach" is different from the traditionally proposed approaches [6–10] in that it does not attempt to individually compute the exergy variations caused by the different factors which may affect any defined thermodynamic system. On the contrary it relies on the unaffected part of the exergy entering and leaving the system [5]. As a result this approach provides the grounds for the non-ambiguous definition of exergy consumed (∇E) and produced (ΔE). As an example of (∇E) and (ΔE) definitions let us analyse the throttling process taking place at sub-environmental conditions. At first let us assume that for this particular case the kinetic energies of the fluid at the inlet and the outlet of the throttling valve are negligible. Then these two quantities are calculated as:

$$\nabla E_{in-tr} = \dot{m} \cdot (e_{in} - e_{tr}) = \dot{m} \cdot [e(P_{in}, T_{in}) - e(P_{out}, T_{in})] = \dot{m} \cdot (\nabla e_P)_{T_{in}} \tag{2}$$

$$\Delta E_{out-tr} = \dot{m} \cdot (e_{out} - e_{tr}) = \dot{m} \cdot [e(P_{out}, T_{out}) - e(P_{out}, T_{in})] = \dot{m} \cdot (\Delta e_T)_{P_{out}} \quad (3)$$

The term $(\nabla e_P)_{Tin}$ in Equation (2) is the decrease of the specific mechanical exergy due to an isothermal pressure drop at constant temperature Tin. The term $(\Delta e_T)_{Pout}$ in Equation (3) is the increase of the specific thermal exergy due to an isobaric temperature drop under sub-environmental conditions at constant pressure Pout. The fluid flow rate is ($\dot{m}$). The specific exergy losses (d) are also presented on the diagram in Figure 2. As illustrated in Equations (4) and (5) the values (∇E) and (ΔE) allow the computation of two important thermodynamic measures, namely exergy efficiency ($\eta_{ex,\,TR}$) and exergy losses (D) where (d) represents the specific exergy losses:

$$\eta_{ex,TR} = \Delta E_{out-tr} / \nabla E_{in-tr} \quad (4)$$

$$D = \dot{m} \cdot d = \nabla E_{in-tr} - \Delta E_{out-tr} \quad (5)$$

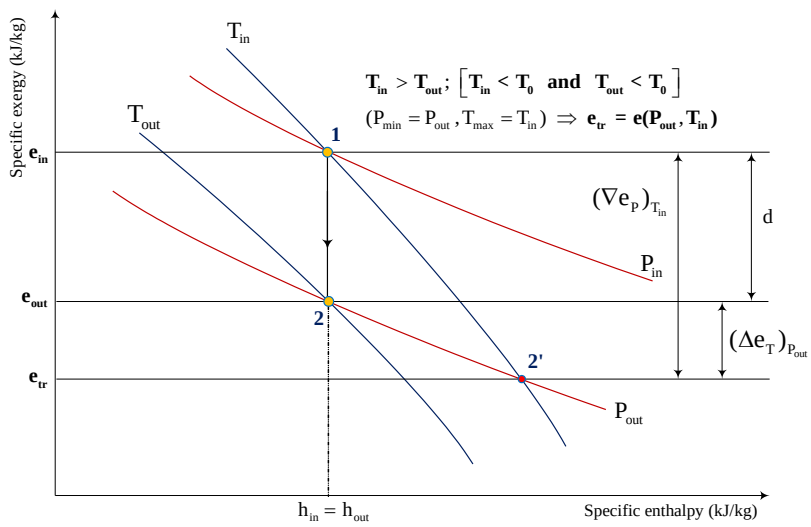

Figure 2. Throttling process on a specific exergy-enthalpy diagram.

The attention of the reader should be drawn to the fact that all the ambiguities, how to define the consumed and produced exergies [5–7], are removed by using the above approach. The values (∇E) and (ΔE) are defined by Equations (2) and (3) in a unique way. The interpretation of the results can be easily represented on the specific exergy-enthalpy diagram presented in Figure 2.

The path 1-2 represents the change occurring to the stream between the throttling valve inlet and outlet conditions. The same overall result could be achieved by following the composite path 1-2′-2. The segment 1-2′ is $(\nabla e_P)_{Tin}$, the segment 2′-2 is $(\Delta e_T)_{Pout}$. Given that the throttling takes place under sub-environmental conditions, the lowest exergy content of the fluid is reached at point 2′ which corresponds to the lowest pressure Pout and the highest temperature Tin. This exergy value is the specific transiting exergy of the stream. If the kinetic energy of the stream cannot be neglected, the lowest velocity value should be added to the definition of transiting exergy as illustrated in Figure 1. The expressions (2) and (3) for consumed and produced exergies will be changed accordingly; the subject is important for an ejector analysis and will be discussed in the next section.

3. The Exergy Consumption and Production in Different Parts of a One-Phase Ejector

The one phase ejector studied in the present paper is the so-called "constant-pressure mixing ejector". It is presented in Figure 3. The exit of the nozzle is located within the suction chamber which is upstream of the constant-area section. The constant-pressure mixing theory of ejector developed by Keenan *et al.* [11] was frequently used in the analysis of constant-pressure ejectors [12,13].

Keenan *et al.* [11] assumed that the primary and the secondary (entrained) flows at the exit of the nozzle have an identical pressure. Mixing of the two streams begins there and proceeds with constant pressure, until the inlet of the constant-area section. This theory is used as one assumption among others in the new validated ejector model [14] that is used in the present paper to calculate the pressure, temperature and velocity at the different cross-sections illustrated in Figure 3. The refrigerant R141b is used as an example for this study. It has been assumed that: the temperature and the pressure of the primary motive fluid entering the primary nozzle are T_4 = 145 °C and P_4 = 1000 kPa, the flow rate is $\dot{m}_p$ = 0.19838 kg/s; the temperature and the pressure of the secondary fluid are T_6 = −5 °C and P_6 = 22.28 kPa, the flow rate is $\dot{m}_s$ = 0.04959 kg/s. According to information compiled by Liu and Groll [15], it has been assumed that the polytropic efficiencies are: 0.95 for the primary nozzle, 0.85 for the suction chamber and 0.78 for the diffuser.

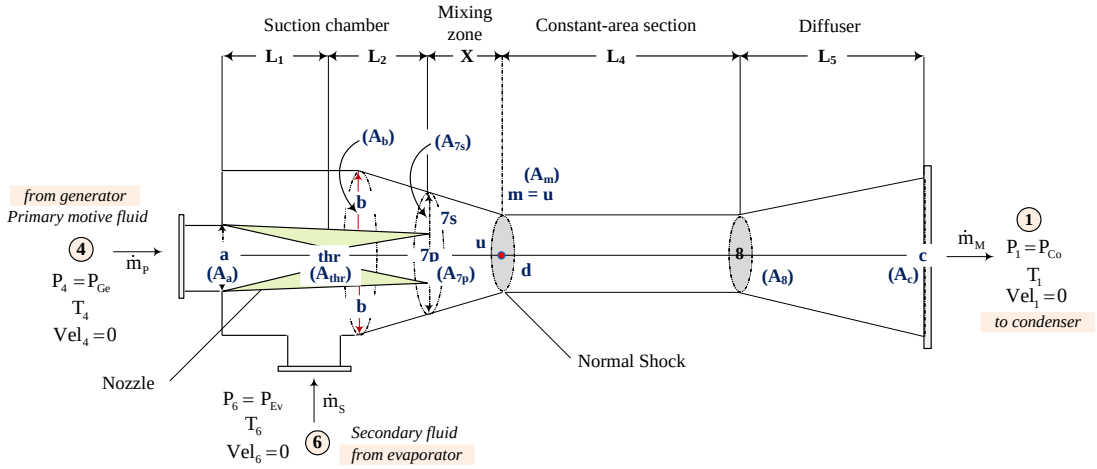

Figure 3. An ejector model with constant mixing pressure.

To make the exergy analysis representative, the ejector is split into 7 sections: (1) primary stream and the converging part of the nozzle (4-thr); (2) diverging part of the nozzle (thr-7p); (3) suction section of the entrained stream (6-7s), (4) mixing zone (7p-m + 7s-m); (5) zone of the shock (m-d); (6) constant area section (d-8); (7) diffuser and the ejector outlet part (8-1). The calculated parameters such as pressure, temperature, velocity and flow-rates at the inlet and outlet of each section are presented in Table 1 [16].

Table 1. Calculated parameters at different ejector's sections with R141b as working fluid.

Fluid	*Primary Fluid*			*Secondary Fluid*		*Mixed Fluid*			
States	4	thr	7p	6	7s	m = u	d	8	1
T (°C)	145.0	125.7	11.2	−5.0	−15.8	16.2	102.9	102.6	106.0
T (K)	418.2	398.9	284.4	268.2	257.4	289.4	376.0	375.7	379.2
P (kPa)	1000.0	603.84	13.06	22.28	13.06	13.06	86.57	83.21	90.84
V (m/s)	0.0	156.2	440.2	0.0	129.2	378.0	73.3	76.2	0.0
M (–)	0.0	0.972	2.956	0.0	0.910	2.517	0.435	0.453	0.0
$\dot{m}$ (kg/s)	0.19838	0.19838	0.19838	0.04959	0.04959	0.24797	0.24797	0.24797	0.24797

The choice of a suitable working fluid is one of the essential steps in the design of the ejector and, subsequently, in the design and manufacturing of the solar driven refrigeration system. Such a fluid must meet the performance criteria as well as the requirements of safety and environmental protection. It must also be available at an affordable price. In the present study, the refrigerant R141b (CH_3CCl_2F) was chosen. Previous studies [17,18] have found that it is suitable for ejector applications. Furthermore, R141b has a positive-slope saturated-vapor line in the temperature-entropy diagram

and therefore does not require superheating. Its critical temperature and pressure are respectively 204.2 °C and 4205 kPa. Its normal boiling point is 32 °C. Its ODP (Ozon depletion potential) value is 0.1 proving that it has a negligible impact on the environment, while its global warming potential (GWP) value is 725 which is quite acceptable for the application under consideration. The profiles of pressure, temperature and velocity along the ejector are illustrated in Figure 4.

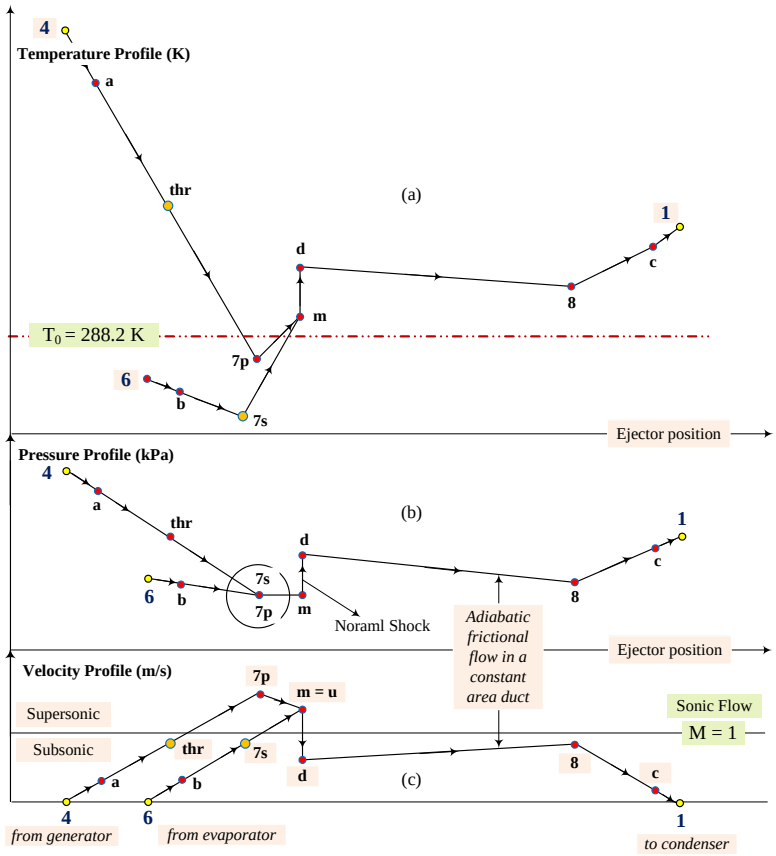

Figure 4. Temperature (**a**), Pressure (**b**) and Velocity (**c**) profiles along the ejector.

By using the definition of transiting exergy from Figure 1 and the simulation results presented in Table 1, it is possible to compute the exergy consumed (∇E) and produced (ΔE) within each part of the ejector. Let us discuss the mathematical expression and the physical meaning of each of these terms.

Section (4-thr):

$$\nabla E_{4-tr} = \dot{m}_p \cdot [e(P_4, T_4, V_4) - e(P_{thr}, T_{thr}, V_4)] = \dot{m}_p \cdot (\nabla e_{P,T}) \quad (6)$$

$$\Delta E_{thr-tr} = \dot{m}_p \cdot [e(P_{thr}, T_{thr}, V_{thr}) - e(P_{thr}, T_{thr}, V_4)] = \dot{m}_p \cdot (\Delta e_V) \quad (7)$$

The exergy consumption is the decrease of thermo-mechanical exergy due to pressure and temperature drops at sup-environmental conditions. The exergy production is the increase of kinetic energy due to the velocity rise from the section's inlet to outlet.

Section (thr-7p):

$$\nabla E_{thr-tr} = \dot{m}_p \cdot \left[e(P_{thr}, T_{thr}, V_{thr}) - e(P_{7p}, T_0, V_{thr})\right] = \dot{m}_p \cdot (\nabla e_{P,T}) \quad (8)$$

$$\Delta E_{7p-tr} = \dot{m}_p \cdot \left[e(P_{7p}, T_{7p}, V_{7p}) - e(P_{7p}, T_0, V_{thr})\right] = \dot{m}_p \cdot \left[(\Delta e_T)_{P_{7p}} + (\Delta e_V)\right] \quad (9)$$

(∇E) is the decrease of thermo-mechanical exergy due to the pressure drop from inlet to outlet and the temperature drop from its inlet value to T_0. The exergy production includes: (1) the increase of thermal exergy due to the temperature drop from T_0 to T_{7p} at the sub-environmental conditions and calculated at constant outlet pressure P_{7p}, and (2) the increase of kinetic energy due to the velocity rise from inlet to outlet.

Section (6-7s):

$$\nabla E_{6-tr} = \dot{m}_s \cdot [e(P_6, T_6, V_6) - e(P_{7s}, T_6, V_6)] = \dot{m}_s \cdot (\nabla e_P)_{T_6} \tag{10}$$

$$\Delta E_{7s-tr} = \dot{m}_s \cdot [e(P_{7s}, T_{7s}, V_{7s}) - e(P_{7s}, T_6, V_6)] = \dot{m}_s \cdot \left[(\Delta e_T)_{P_{7s}} + (\Delta e_V)\right] \tag{11}$$

(∇E) is the decrease of mechanical exergy due to the pressure drop and calculated at constant inlet temperature T_6. (ΔE) is the sum of: (1) the increase of thermal exergy due to the temperature drop in the sub-environmental region and calculated at constant outlet pressure P_{7s}, and (2) the increase of kinetic energy due to the velocity rise from inlet to outlet.

Section (7p-m+7s-m):

$$\begin{aligned}\nabla E_{7p7s-tr} &= \dot{m}_p \cdot \left[e(P_{7p}, T_{7p}, V_{7p}) - e(P_{7p}, T_0, V_m)\right] + \dot{m}_s \cdot [e(P_{7s}, T_{7s}, V_{7s}) - e(P_{7s}, T_0, V_{7s})] \\ &= \dot{m}_p \cdot \left[(\nabla e_T)_{P_{7p}} + (\nabla e_V)\right] + \dot{m}_s \cdot (\nabla e_T)_{P_{7s}}\end{aligned} \tag{12}$$

$$\begin{aligned}\Delta E_{m-tr} &= \dot{m}_p \cdot \left[e(P_m, T_m, V_m) - e(P_{7p}, T_0, V_m)\right] + \dot{m}_s \cdot [e(P_m, T_m, V_m) - e(P_{7s}, T_0, V_{7s})] \\ &= \dot{m}_p \cdot (\Delta e_T)_{P_{7p}} + \dot{m}_s \cdot \left[(\Delta e_T)_{P_{7s}} + (\Delta e_V)\right]\end{aligned} \tag{13}$$

Given that the mixing section deals with two currents ($\dot{m}_p$ and $\dot{m}_s$), the transiting exergies in Equations (12) and (13) are calculated for each current. As a result the consumed exergy is linked to both currents. For the primary stream it is the sum of: (1) the decrease of thermal exergy due to a temperature rise in the sub-environmental region and calculated at constant inlet pressure P_{7p}, and (2) the decrease of kinetic energy due to the velocity reduction. For the secondary stream it is the decrease of thermal exergy due to a temperature rise in the sub-environmental region and calculated at constant inlet pressure P_{7s}. The produced exergy is linked to the primary and secondary streams together. For the primary it is the increase of thermal exergy due to a temperature rise in the sup-environmental region and calculated at constant outlet pressure P_{7p}. For the secondary it is the sum of: (1) the increase of thermal exergy due to the temperature rise in the sub-environmental region and calculated at constant outlet pressure P_{7}s, and (2) the increase of kinetic energy due to the velocity rise.

Figure 5 used the diagram of Grassmann applied to the section (7p-m + 7s-m) to illustrate the existing phenomenon in this mixing zone which is given by the two equations (12) and (13).

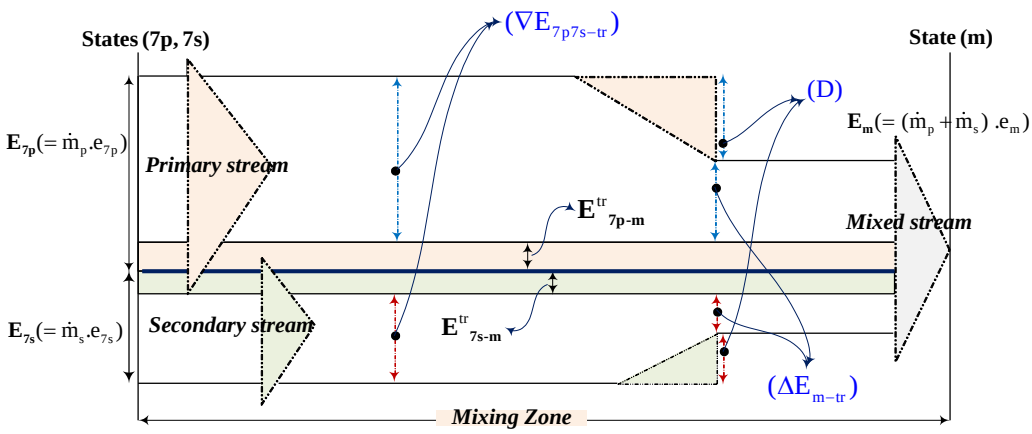

Figure 5. Diagram of Grassman illustrating transiting exergy in the mixing zone.

Section (m-d):

$$\nabla E_{m-tr} = (\dot{m}_p + \dot{m}_s) \cdot [e(P_m, T_m, V_m) - e(P_m, T_m, V_d)] = (\dot{m}_p + \dot{m}_s) \cdot (\nabla e_V) \quad (14)$$

$$\Delta E_{d-tr} = (\dot{m}_p + \dot{m}_s) \cdot [e(P_d, T_d, V_d) - e(P_m, T_m, V_d)] = (\dot{m}_p + \dot{m}_s) \cdot (\Delta e_{P,T}) \quad (15)$$

The exergy consumption (∇E) across the normal shock is the decrease in kinetic energy due to the velocity drop. The exergy production (ΔE) is the increase of thermo-mechanical exergy due to the temperature rise from the inlet to the outlet in sup-environmental region and the increase in pressure from the inlet to the outlet.

Section (d-8):

$$\nabla E_{d-tr} = (\dot{m}_p + \dot{m}_s) \cdot [e(P_d, T_d, V_d) - e(P_8, T_d, V_d)] = (\dot{m}_p + \dot{m}_s) \cdot (\nabla e_P)_{T_d} \quad (16)$$

$$\Delta E_{8-tr} = (\dot{m}_p + \dot{m}_s) \cdot [e(P_8, T_8, V_8) - e(P_8, T_8, V_d)] = (\dot{m}_p + \dot{m}_s) \cdot (\Delta e_V) \quad (17)$$

The temperature variation can be neglected in this section, thus (∇E) is the decrease of mechanical exergy due to the pressure drop caused by friction and calculated at constant inlet temperature T_d. (ΔE) is the increase of kinetic energy due to the velocity rise from the inlet to the outlet.

Section (8-1):

$$\nabla E_{8-tr} = (\dot{m}_p + \dot{m}_s) \cdot [e(P_8, T_8, V_8) - e(P_8, T_8, V_1)] = (\dot{m}_p + \dot{m}_s) \cdot (\nabla e_V) \quad (18)$$

$$\Delta E_{1-tr} = (\dot{m}_p + \dot{m}_s) \cdot [e(P_1, T_1, V_1) - e(P_8, T_8, V_1)] = (\dot{m}_p + \dot{m}_s) \cdot (\Delta e_{P,T}) \quad (19)$$

In this section (∇E) is the decrease in kinetic energy due to the velocity drop. (ΔE) is the increase of thermo-mechanical exergy due to the pressure and temperature rise.

The terms (∇E) and (ΔE) for the overall ejector may be calculated applying the same methodology. Given that the velocities of the stream in the inlet (states 4, 6) and outlet (state 1) of the ejector are negligible, the terms are:

$$\begin{aligned} \nabla E_{46-tr} &= \dot{m}_p \cdot [e(P_4, T_4) - e(P_1, T_1)] + \dot{m}_s \cdot [e(P_6, T_6) - e(P_6, T_0)] \\ &= \dot{m}_p \cdot (\nabla e_{P,T}) + \dot{m}_s \cdot (\nabla e_T)_{P_6} \end{aligned} \quad (20)$$

$$\begin{aligned} \Delta E_{1-tr} &= \dot{m}_p \cdot [e(P_1, T_1) - e(P_1, T_1)] + \dot{m}_s \cdot [e(P_1, T_1) - e(P_6, T_0)] \\ &= \dot{m}_s \cdot (\Delta e_{P,T}) \end{aligned} \quad (21)$$

The consumed exergy is linked to both currents. For the primary stream (∇E) is the decrease of thermo-mechanical exergy due to the pressure and temperature drops in the sub-environmental region. For the secondary stream (∇E) is the decrease of thermal exergy due to the temperature rise from the sub-environmental value to T_0 and calculated at constant inlet pressure P_6. The produced exergy (ΔE) is linked to the secondary stream only. The exergy production is the increase of thermo-mechanical exergy due to the pressure rise from the inlet to the outlet and to the temperature rise from T_0 to T_1.

4. Analysis of Numerical Results

The numerical values of the above terms are presented in Table 2. The corresponding exergy losses (D), Grassmann exergy efficiencies ($\eta_{ex,\,GR}$) and exergy efficiencies taking into account the transition streams ($\eta_{ex,\,TR}$) are calculated according to Equations (1), (4), (5) and are presented in the table as well.

The most important exergy losses take place within the zone of the shock (section m-d). The second important place with the greatest irreversibility is the mixing zone (sections 7p-m + 7s-m). The third one is the diverging part of the nozzle (section thr-7p). Let us now illustrate in which way the newly introduced thermodynamic metrics, exergy consumed (∇E) and produced (ΔE) as well as exergy efficiency ($\eta_{ex,\,TR}$), may be used to complement this analysis.

Table 2. Exergy metrics in different ejector sections.

Section	Exergy Consumed (∇E, kW)	Exergy Produced (ΔE, kW)	Exergy Losses (D, kW)	Transiting Exergy (E^{tr}, kW)	Exergy Efficiency ($\eta_{ex,\,TR}$)	Exergy Efficiency ($\eta_{ex,\,GR}$)
4-thr	2.515	2.421	0.094	11.906	96.3%	99.3%
thr-7p	17.562	16.805	0.757	−3.236	95.7%	94.7%
6-7s	0.539	0.457	0.082	−1.388	84.8%	109.7%
7p-m + 7s-m	5.121	3.130	1.991	7.517	61.1%	84.2%
m-d	17.051	11.764	5.287	−6.404	69.0%	50.3%
d-8	0.211	0.055	0.156	5.149	26.1%	97.1%
8-1	0.721	0.609	0.112	4.483	84.5%	97.9%
total ejector	10.374	1.894	8.480	3.199	18.3%	37.5%

According to Table 2, $D_{m\text{-}d}$ is larger than $D_{7p\text{-}m+7s\text{-}m}$, however $\eta_{m\text{-}d}$ is higher than $\eta_{7p\text{-}m+7s\text{-}m}$. It means that the transformation of thermal and kinetic exergies into thermal and mechanical exergies, taking place within the zone of shock, is thermodynamically more efficient than the transformation of thermal and kinetic exergies into kinetic exergy of the secondary stream, taking place within the zone of mixing. Thus, particular attention should be paid to the improvement of the mixing process. The analysis of expression (12) for (∇E) reveals that the most important factor influencing the irreversible losses in the zone of mixing is the decrease of thermal exergy due to the temperature rise in the sub-environmental region (from 257 K to 289 K for the secondary stream and from 284 K to 289 K for the primary stream). As a result the cold created in the evaporator of a refrigeration system, in the diverging part of the nozzle (thr-7p) and in the suction section of the entrained stream (6-7s) is completely destroyed in the zone of mixing. To our knowledge this type of result has never been published in the scientific literature. The engineering proposals regarding the reduction of (∇E) in this zone and the consequent reduction of exergy losses will be discussed in future publications.

Another important result derived from this analysis deals with the diverging part of the nozzle (thr-7p). As has been already mentioned the exergy losses are substantial in this section. Thus it seems that their reduction is an important direction for the ejector's improvement. However it is not the case. Indeed, the thermodynamic efficiency of the transformation of mechanical and thermal exergies into kinetic and thermal exergies is highly efficient in this section (95.7%). Thus the likelihood of exergy losses reduction here is very low.

Now let's compare the values of Grassman exergy efficiency ($\eta_{ex,\,GR}$) with the efficiency ($\eta_{ex,\,TR}$) taking into account the transiting exergy flow. First of all let's notice that the value of ($\eta_{ex,\,GR}$) for the suction section of the entrained stream (6–7s) is higher than 100%, and thus does not have any physical meaning. The explanation of this unacceptable result is the following; because of the vacuum conditions the exergies E_{7s} and E_6 are negative, where E_{7s} is lower than E_6 by the value of exergy losses. It means that absolute value of E_{7s} is higher than E_6. As a result the ratio E_{7s}/E_6 is higher than 1. Contrary to ($\eta_{ex,\,GR}$), the value of ($\eta_{ex,\,TR}$) is lower than 100%, and it reflects in this way the exergy losses occurring within the suction section of the entrained stream.

The second observation concerns the efficiencies of the mixing zone (7p-m + 7s-m) and the zone of the shock (m-d). According to ($\eta_{ex,\,GR}$) the section (m-d) is less efficient and according to ($\eta_{ex,\,TR}$) it is more efficient. The main reason of this contradiction is the fact that exergy flows at the entries and exists of each zone present the summation of positive terms (thermal and kinetic exergies) and negative ones (mechanical exergies under vacuum conditions). As a result their ratio ($\eta_{ex,\,GR}$) does reflect the mutual transformation of one form of exergy to another. On the contrary, given that the transiting part of mechanical exergy is negative, the application of ($\eta_{ex,\,TR}$) reflects this mutual transformation. Thus by transforming the kinetic exergy to mechanical one, the zone of the shock is more efficient than the mixing zone. The third observation concerns the constant area section (d-8). According to ($\eta_{ex,\,TR}$), it is the less efficient part of the ejector. According to ($\eta_{ex,\,GR}$), it is one of the most efficient. The main

reason of this discrepancy is the presence of an important transiting exergy flow; this fact is ignored when the Grassman exergy efficiency is applied.

Finally the exergy efficiency ($\eta_{ex,\,TR}$) of the overall ejector, calculated according to Equations (20), (21) and (4) is low and equals 18.3%, contrary to the "optimistic" value 37.5% of ($\eta_{ex,\,GR}$). The main reason of this difference is the presence of an important transiting exergy flow of 3.2 kW.

5. Conclusions

Calculation of the transiting exergy within different sections of a one phase ejector allows the evaluation of two thermodynamically important metrics, exergy produced and exergy consumed. Their application permitted the evaluation of the mutual transformation of different kinds of exergy linked to three intensive parameters of the flow inside the ejector, namely pressure, temperature and velocity. One of the lowest thermodynamic efficiencies takes place in the mixing zone. The most important factor responsible for this is the temperature rise in the sub-environmental region. Grassmann exergy efficiency is not an appropriate criterion for evaluation of ejectors thermodynamic performance.

Acknowledgments: This project is a part of the Collaborative Research and Development (CRD) Grants Program at "Université de Sherbrooke". The authors acknowledge the support of the Natural Sciences and Engineering Research Council of Canada, Hydro Québec, Rio Tinto Alcan and CanmetENERGY Research Center of Natural Resources Canada.

Author Contributions: This paper is the result of the work of all the authors. Mohammed Khennich, principal investigator developed the ejector model. Mikhail Sorin proposed the methodology of transiting exergy and provided guidance as well as technical assistance. Nicolas Galanis provided scientific and technical assistance. All authors contributed to the discussion of the results.

Conflicts of Interest: The authors declare no conflict of interest.

Abbreviations

The following abbreviations are used in this manuscript:

Symbols		Greek Symbols	
A	Area, cm^2	η	Efficiency, %
Co	Condenser	∇	Thermodynamic metric: consumption
D	Destroyed exergy, kW	Δ	Thermodynamic metric: production
d	Specific exergy losses, kJ/kg		***Subscripts***
E	Exergy, kW	0	Dead state
e	Specific exergy, kJ/kg	4, thr,	States in one phase ejector
Ev	Evaporator	d	Downstream
Ge	Generator	in	Inlet
h	Specific enthalpy, kJ/kg	M, m	Mixing
L	Ejector part's length, cm	max	Maximal
M	Mach number	min	Minimal
$\dot{m}$	Mass flowrate, kg/s	out	Outlet
P	Pressure, kPa	p	Primary
T	Temperature, °C, K	s	Secondary
V	Velocity, m/s	thr	Throat
X	Ejector part's length, cm	tr	Transiting

References

1. Chen, X.; Omer, S.; Worall, M.; Riffat, S. Recent developments in ejector refrigeration technologies. *Renew. Sustain. Energy Rev.* **2013**, *19*, 629–651. [CrossRef]
2. Arbel, A.; Shklyar, A.; Hershgal, D.; Barak, M.; Sokolov, M. Ejector irreversibility characteristics. *J. Fluid Eng.* **2003**, *125*, 121–129. [CrossRef]

3. Al-Najem, N.M.; Darwish, M.A.; Youssef, F.A. Thermovapor compression desalters: Energy and availability—Analysis of single- and multi-effect systems. *Desalination* **1997**, *110*, 223–238. [CrossRef]
4. McGovern, R.K.; Narayan, G.P.; Lienhard, V.J.H. Analysis of reversible ejectors and definition of an ejector efficiency. *Int. J. Therm. Sci.* **2012**, *54*, 153–166. [CrossRef]
5. Brodyansky, V.M.; Sorin, M.; LeGoff, P. *The Efficiency of Industrial Processes: Exergy Analysis and Optimization*; Elsevier Science B. V: Amsterdam, The Netherlands, 1994.
6. Kotas, T.J. *The Exergy Method of Thermal Plant Analysis*, 2th ed.; Krieger Publishing: Malabar, FL, USA, 1995.
7. Marmolejo-Correa, D.; Gundersen, T. A comparison of exergy efficiency definitions with focus on low temperature processes. *Energy* **2012**, *44*, 477–489. [CrossRef]
8. Zanchini, E. A more general exergy function and its application to the definition of exergy efficiency. *Energy* **2015**, *87*, 352–360. [CrossRef]
9. Lazzaretto, A.; Tsatsaronis, G. SPECO: A systematic and general methodology for calculating efficiencies and costs in thermal systems. *Energy* **2006**, *31*, 1257–1289. [CrossRef]
10. Lior, N.; Zhang, N. Energy, exergy, and Second Law performance criteria. *Energy* **2007**, *32*, 281–296. [CrossRef]
11. Keenan, H.; Neumann, E.P.; Lustwerk, F. An investigation of ejector design by analysis and experiment. *J. Appl. Mech. Trans. ASME* **1950**, *72*, 299–309.
12. Sun, D.W.; Eames, I.W. Performance characteristics of HCFC-123 ejector refrigeration cycles. *Int. J. Energy Res.* **1996**, *20*, 871–885. [CrossRef]
13. Sun, D.W. Experimental investigation of the performance characteristics of a steam jet refrigeration system. *Energy Sources* **1997**, *19*, 349–367. [CrossRef]
14. Khennich, M.; Galanis, N.; Sorin, M. Effects of design conditions and irreversibilities on the dimensions of ejectors in refrigeration systems. *Appl. Energ.* **2016**. submitted.
15. Liu, F.; Groll, E.A. Study of ejector efficiencies in refrigeration cycles. *Appl. Therm. Eng.* **2013**, *52*, 360–370. [CrossRef]
16. Khennich, M.; Sorin, M.; Galanis, N. Effects of condenser pressure on the size and operation conditions of ejector refrigeration systems. In Proceedings of the International Conference on Innovative Technologies (INTECH), Dubrovnik, Croatia, 9–11 September 2015.
17. Huang, B.J.; Chang, J.M. Empirical correlation for ejector design. *Int. J. Refrig.* **1999**, *22*, 379–388. [CrossRef]
18. Dorantes, R.; Lallemand, A. Prediction of performance of a jet cooling system operating with pure refrigerants or non-azeotropic mixtures. *Int. J. Refrig.* **1995**, *18*, 21–30.

© 2016 by the authors; licensee MDPI, Basel, Switzerland. This article is an open access article distributed under the terms and conditions of the Creative Commons by Attribution (CC-BY) license (http://creativecommons.org/licenses/by/4.0/).